ICARUS 57, 356–361 (1984)

Venus Zonal Wind above the Cloud Layer

R. S. LINDZEN* AND H. TEITELBAUM†

*Department of Earth, Atmospheric and Planetary Sciences, Massachusetts Institute of Technology, Cambridge, Massachusetts 02139, and †Laboratoire de Météorologie Dynamique du CNRS, Ecole Polytechnique, 91128 Palaiseau Cedex, France

Received July 25, 1983; revised December 13, 1983

The altitude variation of the zonal wind velocity in the Venus atmosphere above the cloud layer is deduced from the structure of the wavenumber 2 solar tide. Results show that the amplitude of the zonal wind increases with respect to altitude near the equator, but decreases for latitudes greater than 30°. Thus, the zonal wind becomes concentrated at lower latitudes by 100 km altitude.

INTRODUCTION

Very important progress on the structure of the mean zonal wind in the Venus atmosphere has been made from the data provided by the Pioneer Venus experiment.

The result obtained with the DLBI (differential long-baseline interferometry) experiment gives a retrograde zonal wind speed of at least 100 m/sec at the top cloud level (≃65 km) (Counselman *et al.*, 1980). From this level and up to 100 km, the mean zonal wind has been deduced from cyclostrophic balance. The equator to pole temperature variation used in these calculations comes from measurements made by the OIR (orbiter infrared radiometer) experiment (Taylor *et al.*, 1979); orbiter occultation (Kliore and Pater, 1980) and probe entry data (Seiff *et al.*, 1980).

With these temperature data and invoking cyclostrophic balance, Shubert *et al.* (1980) found a maximum of wind velocity of 160 and 140 m/sec at 65 and 95 km altitude, respectively. Above 95 km, the wind amplitude decreases abruptly. Seiff (1982) after an analysis of the data concludes that an altitude of 85 km is the better estimate for the near-zero velocity level.

In this paper, we shall reexamine these results in the light of the structure of the wavenumber 2 solar tide, as Schofield and Taylor (1983) have analyzed it from data.

CALCULATION OF THE MEAN ZONAL WIND VELOCITY

The phase variation of the wavenumber 2 solar tide plotted in solar fixed coordinates shows, near the equator, a strong decrease of the vertical wavelength at 86 km altitude coincident with a decrease in amplitude. Another not so strong decrease in wavelength is shown at 72 km (See Fig. 1).

Such an oscillation in wavelength—having itself a wavelength equal to half the average wavelength—is generally indicative of the interference pattern formed by an upward propagating wave and a weaker downward propagating wave, each having the average wavelength. The alternative interpretation of a pure upward traveling wave which happens to have an oscillation in local wavelength with a wavelength equal to half that of the average wavelength is unlikely. The interference effect is described in the Appendix. The upward propagating wave must be mainly generated by the SO_2 and aerosol heating about 65 km altitude (Teitelbaum and Cot, 1981). The downward propagating wave might be due to another source or a reflecting mechanism at higher altitude.

We shall first deduce the mean zonal wind, by admitting the existence of the downward propagating wave and using the interference pattern to deduce the average

0019-1035/84 $3.00

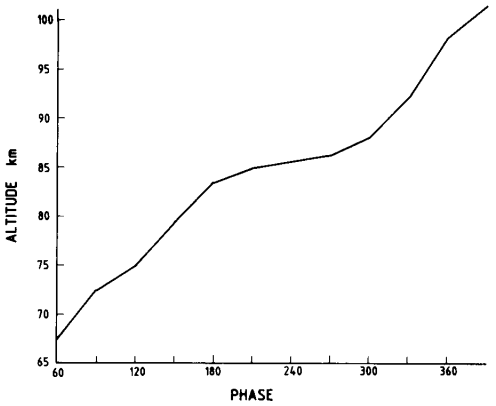

FIG. 1. Phase variation of the wavenumber 2 solar tide at the equator (after Schofield and Taylor).

wavelength. We next evaluate the average wavelengths directly without reference to the interference pattern.

While the question of what if anything is causing the downward propagating wave, is still open, the average wavelength itself is a good indicator of the zonal wind. The point here is the following: for tidal modes (and other waves for that matter), the dispersion relation relates local vertical wavelength to thermal structure, horizontal wavenumber (largely determined by forcing), and most importantly, the phase speed of the forcing relative to the atmospheric zonal flow. We will discuss the dispersion relation later in this paper. However, for the moment it should be noted that for the Earth, this phase speed for thermal tides is largely determined by the rotation rate of the Earth. On the other hand, for Venus it is almost totally indicative of the zonal flow of the atmosphere. It is in the nature of the shape of the main semidiurnal mode that it emphasizes zonal winds near the equator. This too will be discussed later. We may reasonably associate zonal wavenumber 2 perturbations on Venus with the main (first) semidiurnal mode. In the Earth's mesosphere, the main semidiurnal mode is trapped allowing higher order modes to assume greater importance (Lindzen & Hong, 1974). Such trapping does not occur in Venus' atmosphere.

If we assume there is a downward propagating wave, then we can infer mean vertical wavelengths from the oscillations in phase progression. This leads to a vertical wavelength of 28 km between 72 and 86 km. Between 86 and 102 km, the wavelength seems to be 32 km. Alternatively, we may consider a lower layer where the phase varies from 60 to 120° implying an average wavelength of 35 km. Similarly, in an upper layer where the phase varies from 120 to 30°, the average wavelength is also 35 km. Differences almost certainly represent uncertainties in the estimates of vertical wavelengths. However, even such coarse estimates provide useful information.

Our procedure will be to evaluate the relation between vertical wavelength and the zonally averaged zonal velocity and temperature, $\bar{u}(z)$ and $\bar{T}(z)$, from the wave dispersion relation. Figure 2, which shows inferred amplitude vs height, presents a secondary feature of some interest. Theory suggests that in the absence of any wave dissipation, wave amplitude should increase with height roughly in inverse proportion to the square root of the unperturbed pressure. Clearly, amplitudes in Fig. 2 remain almost constant with height. We cannot dismiss the possibility that this constancy is partially an artifact of the data analysis. However, assuming the con-

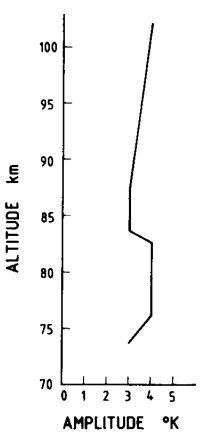

FIG. 2. Amplitude variation of the wavenumber 2 solar tide at the equator (after Schofield and Taylor).

stancy of amplitude with height is real, we are able to estimate the damping time scale by parameterizing the damping in terms of linear friction (Rayleigh friction) and linear thermal damping (Newtonian cooling). If we take the damping time for each to be the same, then the inclusion of such damping amounts simply to allowing an imaginary component of frequency. By choosing the imaginary component to cancel the expected amplitude growth with height, we obtain a rough time scale associated with processes damping the tide. No physical mechanism is specifically identified for this damping, though if one assumes it is due to eddy diffusion, a diffusion coefficient may be inferred. Support for the existence of substantial damping comes from the oscillation in local vertical wavelength. In the Appendix we show that the amplitude of the oscillation is determined by the ratio of downward to upward propagating waves. At 86 km this ratio is estimated to be about 0.5 while at 72 km it is much smaller. This is consistent with the damping of both wave components. Finally, it should be stated that the damping we find, while large, does not prove very significant in its effect on the vertical phase progression. Completely ignoring damping alters estimates of $\bar{u}$ by less than 20%—leading, in fact, to larger values of $\bar{u}$ than those given here.

From classical tidal theory (Chapman and Lindzen, 1970), we have a local complex vertical wavenumber given by

$$K_z = \left\{\frac{1}{hH}\left(\kappa + \frac{dH}{dz}\right) - \frac{1}{4H^2}\right\}^{1/2} \quad (1)$$

where

$H = \dfrac{RT}{g}$

z = altitude

$\kappa = \dfrac{\gamma - 1}{\gamma}$

$\gamma = 1.3$

h = equivalent depth.

From observations, we have K_z. (Note: if K_z were real, amplitudes would be increasing as $\exp(z/2H)$; constancy of amplitude requires an imaginary component of K_z.) Our choice for H and dH/dz in the upper and lower regions is based on the temperature profile in Seiff *et al.* (1979). Thus, (1) can be solved for the complex equivalent depth, h.

If one assumes that the mean flow at each level consists in constant angular velocity characterized by the zonal velocity at the equator, $\bar{u}$, then one may solve Laplace's tidal equation to obtain the complex frequency associated with the observationally deduced h. Alternatively, one might use the extensive tabulations of Longuet-Higgins (1967). For our purposes we have found it easier and about as accurate to use the analytic results for an equatorial β plane (Lindzen, 1967). The dispersion relation can be written as

$$\varepsilon \frac{\hat{\sigma}^3}{8\hat{\Omega}^3} - S^2 \frac{\hat{\sigma}}{2\hat{\Omega}} - \frac{(2n+1)\hat{\sigma}}{2\hat{\Omega}} \varepsilon^{1/2} + S = 0 \quad (2)$$

where

$\hat{\sigma} = S(\Omega_v + \Omega_o + \bar{u}/a) - i\alpha$

$\hat{\Omega} = \Omega_v + \bar{u}/a$

$\Omega_v = 3 \times 10^{-7}\ S^{-1}$ sidereal frequency

$\Omega_o = 2.23 \times 10^{-7}\ S^{-1}$ frequency about the sun

$S = 2;\ n = 1$

$\varepsilon = (2\hat{\Omega}a)^2/gh$

$a = 6120$ km distance from Venus center

$g = 8.6$ m sec^{-2} gravity

h = equivalent height (complex)

$\bar{u}$ = mean zonal wind at the equator.

Given h, (2) can be solved for $\bar{u}$ and α. The results are shown in Table I. Also shown are the diffusivities implied by α if we assume damping is due to turbulent diffusion, i.e.,

$$K = \alpha/K_z^2.$$

Several items in Table I warrant further comments:

(i) The inferred values of damping are large. The values of α are much larger than those expected from infrared cooling (Dickinson, 1972). Similarly, the values of K are larger than those derived by Winnick and Stewart (1980) from the SO_2 budget (i.e., $K = 2 \times 10^4$ cm^2 sec^{-1} at 65 km) or by Von Zahn *et al.* (1980) ($K = 2 \times 10^5$ cm^2 sec^{-1} at 100 km). We can give two possible explanations for these discrepancies: (a) The wave can be damped by mechanisms other than turbulence. (b) In the layer between 70 and 100 km, the variation of K can be different than the one given by Von Zahn *et al.* (1980) leading to higher intermediate values.

(ii) Our results suggest an increase in $\bar{u}$ from the lower to the upper layer in contrast to the findings of Schubert *et al.* (1980) and Seiff (1982) whose results suggested a sharp diminution of $\bar{u}$ above about 94 km. However, the techniques used by Schubert *et al.* (1980) and Seiff (1982) both emphasize higher latitudes. Seiff (1982) used a weighted mean over latitude with weighting favoring higher latitudes. Schubert *et al.* (1980) used the cyclostrophic relation; however, in cyclostrophic balance, equatorial winds are sensitive to unmeasurably small variations in pressure gradient.

Tidal behavior, on the other hand, emphasizes the tropical basic state. Our results would be consistent with earlier results if the decrease of $\bar{u}$ above 94 km occurred poleward of about 30° latitude. The observation of more rapid phase progression at higher latitudes (Schofield and Taylor, 1983) may be compatible with this hypothesis.

To test qualitatively this hypothesis we have performed two nonseparable, numerical calculations with the method of Lindzen and Hong (1974). This method allows us to consider zonal winds which vary with altitude and latitude.

TABLE I

	H (km)	$\frac{dH}{dZ}$	Interference method					Averaging method				
			Vertical wavelength (km)	h(complex) (km)	$\bar{u}$ (m sec^{-1})	$\alpha \times 10^5$ (sec^{-1})	$K \times 10^{-6}$ (cm^2 sec^{-1})	Vertical wavelength (km)	h(complex) (km)	$\bar{u}$ (m sec^{-1})	$\alpha \times 10^5$ (sec^{-1})	$K \times 10^{-6}$ (cm^2 sec^{-1})
Upper region (86–100 km)	4.3	3×10^{-2}	32	(0.5; −0.54)	128	1.3	3.4	35	(0.54; −0.7)	135	1.35	4.2
Lower region (72–86 km)	5	5×10^{-2}	28	(0.4; −0.35)	108	0.85	1.7	35	(0.5; −0.55)	126	1.16	3.6

In the first calculation, the zonal wind velocity is taken as independent of altitude with constant angular velocity. The result shows phase progression independent of latitude.

In the second calculation, we take, above 75 km, a zonal wind decreasing with respect to altitude for latitudes greater than 30°. In this case, the phase progression is faster in latitudes greater than 30°; results at the equator are only weakly affected.

CONCLUSION

We conclude that the zonal wind velocity which in the cloud layer is nearly a "solid body" rotation (Limaye *et al.*, 1982) becomes concentrated at lower latitudes by 100 km altitude.

APPENDIX

The temperature perturbation induced by an upward propagating wave can be written as

$$\Delta T_u = Ae^{(1/2H-\mu)z}\cos(\sigma t + S\phi + k_z z) \tag{A-1}$$

and that induced by a downward propagating wave as

$$\Delta T_d = ARe^{(1/2H+\mu)z}\cos(\sigma t + S\phi - k_z z + \delta) \tag{A-2}$$

where

σ = wave frequency
S = zonal wavenumber
k_z = vertical wavenumber
μ = coefficient of the expontial variation of amplitude due to dissipation
A = amplitude of the upward propagating wave
R = amplitude ratio between the downward and the upward propagating waves
δ = phase difference between upward and downward propagating waves.

A and R are so defined at a given altitude, say $z = 0$. The interpretation of R at a different altitude is no longer correct because of damping; the correct ratio is, however, easily calculated. Rearranging terms, the total temperature perturbation can be written as

$$AB(z)e^{(1/2H-\mu)z}\cos(\sigma t + S\varphi + \Psi(z))$$

where

$$B(z) = (1 + R^2C^{4\mu z} + 2Re^{2\mu z}\cos(2k_z z - \delta))^{1/2} \tag{A-3}$$

and

$$\Psi(z) = \operatorname{arctg}\frac{\sin k_z z - Re^{2\mu z}\sin(k_z z - \delta)}{\cos k_z z + Re^{2\mu z}\cos(k_z z - \delta)}. \tag{A-4}$$

The phase progression is given by

$$\frac{d\Psi(z)}{dz} = \frac{k_z(1 - R^2e^{4\mu z}) - 2\mu Re^{2\mu z}\sin(2k_z z - \delta)}{1 + R^2e^{4\mu z} + 2Re^{2\mu z}\cos(2k_z z - \delta)}. \tag{A-5}$$

The maxima of phase progression are near levels where $\cos(2k_z z - \delta) = -1$, with magnitude

$$\frac{d\Psi}{dz} \simeq k_z\left(\frac{1 + Re^{2\mu z}}{1 - Re^{2\mu z}}\right). \tag{A-6}$$

The last two expressions show that (1) the maxima are separated by a half vertical wavelength; (2) the magnitude of the maxima is decreasing when the altitude is lower, as a consequence of the damping process.

ACKNOWLEDGMENTS

The work of R. S. Lindzen is supported by NASA Grant NGL 22-007-228 and NSF Grant ATM 82-05638.

REFERENCES

CHAPMAN, S., AND R. S. LINDZEN (1970). *Atmospheric Tides*. Gordon & Breach/Science, New York.

COUNSELMAN, C. C., III, S. A. GOUREVITCH, R. W. KING, G. B. LORIOT, AND E. S. GINSBERG (1980). Zonal and meridional circulation of the lower atmosphere of Venus determined by radio interferometry. *J. Geophys. Res.* **85,** 8026–8030.

DICKINSON, R. E. (1972). Infrared radiative heating and cooling in the Venusian mesosphere. I: Global mean radiative equilibrium. *J. Atmos. Sci.* **29,** 1531–1556.

KLIORE, A. J., AND I. R. PATEL (1980). Verticle structure of the atmosphere of Venus from Pioneer Venus orbiter radio occultation. *J. Geophys. Res.* **85,** 7985–7962.

LIMAYE, S. S., J. G. CHRISTIAN, AND S. P. BURRE (1982). Zonal mean circulation at the cloud level on Venus: Spring and Fall 1979 OCPP observations. *Icarus* **51,** 416–439.

LINDZEN, R. S. (1967). Planetary waves on beta-planes. *Mon. Weather Rev.* **95,** 441–451.

LINDZEN, R. S., AND J. FORBES (1983). Turbulence originating from convectively stable internal waves. *J. Geophys. Res.* **88,** 6549–6553.

LONGUET-HIGGINS, M. S. (1967). The eigenfunction of Laplace's tidal equations over a sphere. *Philos. Trans. Roy. Soc.* **109,** 511–607.

SCHOFIELD, J. T., AND F. W. TAYLOR (1983). Measurements of the mean, solar-fixed temperature and cloud structure of the middle atmosphere of Venus. *Quart. J. Roy. Meteorol. Soc.* **109,** 57–80.

SCHUBERT, G., C. O. COVEY, A. DEL GENIO, L. S. ELSON, G. KEATING, A. SEIFF, R. E. YOUNG, J. APT, C. C. COUNSELMAN, III, A. K. KLIORE, S. S. LIMAYE, H. E. REVERCOMB, L. A. SROMOVSKY, V. E. SUOMI, F. TAYLOR, R. WOO, AND U. VON ZAHN (1980). Structure and circulation of the Venus atmosphere. *J. Geophys. Res.* **85,** 8007–8025.

SEIFF, A., D. B. KIRK, R. E. YOUNG, S. C. SOMMER, R. C. BLANCHARD, J. T. FINDLAY, AND G. M. KELLEY (1979). Thermal contrast in the atmosphere of venus: Initial appraisal from Pioneer Venus probe data. *Science* **205,** 46–49.

SEIFF, A., D. B. KIRD, R. E. YOUNG, R. C. BLANCHARD, J. T. FINDLAY, G. M. KELLY, AND S. C. SOMMER (1980). Measurements of thermal structure and thermal contrast in the atmosphere of Venus and related dynamical observations: Results from the Four Pioneer Venus probes. *J. Geophys. Res.* **85,** 7903–7933.

SEIFF, A. (1982). Dynamical implications of the observed thermal contrast in Venus upper atmosphere. *Icarus* **51,** 574–592.

TAYLOR, F. W., D. J. DINER, L. S. ELSON, D. J. MCCLEESE, J. V. MARTONCHIK, J. DELDERFIELD, S. P. BRADLEY, J. T. SCHOFIELD, J. C. GILLE, AND M. T. COFFEY (1979). Temperature, cloud structure, and dynamics of Venus middle atmosphere by infrared remote sensing from Pioneer orbiter. *Science* **205,** 65–67.

TEITELBAUM, H., AND C. COT (1981). Calculation of the solar gravitational torque on the Venus thermal tide. *Astron. Astrophys.* **97,** 265–268.

VON ZAHN, U., K. H. FRICKE, D. M. HUNTEN, D. KRANKOVSKY, K. MAUERSBERGER, AND A. O. NIER (1980). The upper atmosphere of Venus during morning conditions. *J. Geophys. Res.* **85,** 7829–7840.

WINNICK, J. R., AND A. I. F. STEWART (1980). Photochemisty of SO_2 in Venus upper cloud layers. *J. Geophys. Res.* **85,** 7849–7860.